Vectorial FDTD Technique for the Analysis of Optical Second-Harmonic Generation

Mohammad A. Alsunaidi, Husain M. Al-Mudhaffar, and Husain M. Masoudi

***Abstract*—A vectorial time-domain simulator of integrated optical structures containing second-order nonlinearities has been formulated and tested. The technique is based on the direct time-domain representation of the coupled nonlinear Maxwell's equations of the propagating fields. The proposed algorithm accounts for the full optical coefficient tensor, input depletion, and device-wave interactions, where the inaccuracies associated with the scalar and paraxial approximations are avoided. Error analysis associated with the proposed scheme is also given. The proposed model should find application in a wide range of device structures and also in the analysis of short-pulse propagation in second-order nonlinear devices.**

***Index Terms*—Finite-difference time-domain (FDTD) method, integrated optics, optical waveguides, second-harmonic generation (SHG), second-order nonlinearity.**

I. Introduction

THE design cycle of modern photonic devices can be shortened considerably by the utilization of accurate device models. The need for accurate device models has never been so great, especially with the increased progress in materials technology and fabrication methods. Fortunately, the availability of fast and powerful computers has made detailed numerical simulation an efficient and reliable tool for researchers and engineers. Accurate analytical models of nonlinear devices, however, are extremely difficult to obtain, and so several numerical methods have been proposed and developed. One of the early methods to be used in nonlinear integrated optics simulation is the beam propagation method [1] with a recent extension to vectorial applications developed in [2]. This method is relatively computationally efficient, but it is aimed at modeling wave propagation in devices where the primary flow of energy is along a single principal direction. Other modeling methods in this area include the finite-element method [3] and the finite-difference time-domain (FDTD) method [4]–[7]. The FDTD is substantially more robust than other methods because it directly solves for fundamental quantities. It also avoids the simplifying assumptions of conventional asymptotic behavior and paraxial propagation. The time-domain nature of the method allows for a number of useful analyses including transient analysis, reflections, time-pulse applications, and temporal nonlinear effects. In most practical nonlinear integrated optical devices, wave polarization does occur and the vector nature of the propagating fields is important. The previously reported vectorial FDTD algorithms for second-order nonlinearity introduce an additional step in the solution where the relationship between the electric flux density and the electric field is employed. This procedure results in a mixed implicit–explicit FDTD scheme that is solved by iteration. The combined expression for the total field, as in [7], is problematic. It works only when the field components of the pump input and the generated waves are separable: a fact that makes such approaches lose generality. Occasionally, input depletion is ignored to relax the strong coupling inherent in the problem. In this letter, an alternative formulation of the full-wave model for second-harmonic generation (SHG) in optical structures containing second-order nonlinearity is presented. In this formulation, a set of field equations is introduced for individual waves (fundamental and second harmonic) with appropriate nonlinear coupling. The algorithm is useful in the analysis of nonlinear effects in many optical structures and for arbitrary input conditions including pulsed inputs.

Manuscript received November 03, 2008; revised November 24, 2008. First published January 06, 2009; current version published February 19, 2009 . This work was supported by King Fahd University of Petroleum and Minerals.

The authors are with the Electrical Engineering Department, King Fahd University of Petroleum and Minerals, Dhahran 31261, Saudi Arabia (e-mail: msunaidi@kfupm.edu.sa; hussein_mm@hotmail.com; husainm@kfupm.edu.sa).

Digital Object Identifier 10.1109/LPT.2008.2010869

II. Formulations

The propagation of electromagnetic radiation through certain class of crystals causes the nonlinear dielectric properties of the material to be polarized. This polarization P can be expressed mathematically using terms proportional to the nonlinear susceptibility $\chi^{(2)}$ and to the propagating electric field components inside the structure. The nonlinear response of the material to such property leads to an exchange of energy between fields propagating at different frequencies. This response is utilized in the SHG in which energy from one field propagating at frequency ω_f, the fundamental field, is transferred to a field propagating at double the frequency ($\omega_s = 2\omega_f$), the second-harmonic field. The linear and nonlinear polarizations are expressed, respectively, as

$$P^L = \varepsilon_o \left([\varepsilon_r] - 1\right) E \tag{1}$$

$$P^{NL} = 2\varepsilon_o [d] E \cdot E \tag{2}$$

where the nonlinear optical coefficient tensor is given by

$$[d] = \begin{bmatrix} d_{11} d_{12} d_{13} d_{14} d_{15} d_{16} \\ d_{21} d_{22} d_{23} d_{24} d_{25} d_{26} \\ d_{31} d_{32} d_{33} d_{34} d_{35} d_{36} \end{bmatrix}. \tag{3}$$

In vectorial form, the nonlinear polarization of the fundamental and the second-harmonic waves are given, respectively, by

$$\begin{bmatrix} P_x^{NL,f} \\ P_y^{NL,f} \\ P_z^{NL,f} \end{bmatrix} = 2\varepsilon_o[d] \begin{bmatrix} E_x^f E_x^s \\ E_y^f E_y^s \\ E_z^f E_z^s \\ E_z^f E_y^s + E_y^f E_z^s \\ E_z^f E_x^s + E_x^f E_z^s \\ E_x^f E_y^s + E_y^f E_x^s \end{bmatrix} \tag{4}$$

and

$$\begin{bmatrix} P_x^{NL,s} \\ P_y^{NL,s} \\ P_z^{NL,s} \end{bmatrix} = \varepsilon_o[d] \begin{bmatrix} E_x^f E_x^f \\ E_y^f E_y^f \\ E_z^f E_z^f \\ 2E_z^f E_y^f \\ 2E_x^f E_z^f \\ 2E_x^f E_y^f \end{bmatrix}. \tag{5}$$

For the sake of illustration and without loss of generality, 2-D GaAs-based waveguides with crystal axes matching the principal axes are considered. In this case, the only nonzero elements in the nonlinear optical coefficient tensor are d_{14}, d_{25}, and d_{36}. Upon inspection of (4) and (5) and setting $d_{14} = d_{25} = d_{36}$, Maxwell's nonlinear equations for the fundamental field and the generated second-harmonic field can be written, respectively, as

$$\varepsilon_x \frac{\partial E_x^f}{\partial t} = -\frac{\partial H_y^f}{\partial z} - 2\varepsilon_o d_{14} \frac{\partial}{\partial t}\left(E_z^f E_y^s\right) \tag{6}$$

$$\varepsilon_z \frac{\partial E_z^f}{\partial t} = \frac{\partial H_y^f}{\partial x} - 2\varepsilon_o d_{14} \frac{\partial}{\partial t}\left(E_x^f E_y^s\right) \tag{7}$$

$$\mu \frac{\partial H_y^f}{\partial t} = \frac{\partial E_z^f}{\partial x} - \frac{\partial E_x^f}{\partial z} \tag{8}$$

and

$$\varepsilon_y \frac{\partial E_y^s}{\partial t} = \left(\frac{\partial H_x^s}{\partial z} - \frac{\partial H_z^s}{\partial x}\right) - 2\varepsilon_o d_{14} \frac{\partial}{\partial t}\left(E_x^f E_z^f\right) \tag{9}$$

$$\mu \frac{\partial H_x^s}{\partial t} = \frac{\partial E_y^s}{\partial z} \tag{10}$$

$$\mu \frac{\partial H_z^s}{\partial t} = -\frac{\partial E_y^s}{\partial x}. \tag{11}$$

III. Simulation Results

The time and space derivatives in the model equations are approximated using the usual leap-frog scheme. For example, the update equation for the second-harmonic y-component of the electric field is given by (12), shown at the bottom of the page, where $T^n = E_x^{f(n)} E_z^{f(n)}$. It should be noted here that, in the general full-wave case when more nonzero elements exist in the d tensor, the computation algorithm is still valid. However, more computations will be needed for the evaluation of the coefficients of the FDTD equations. For example, in (12), five more terms will appear in the nonlinear polarization part involving E_x^f, E_y^f, and E_z^f. To increase the accuracy of the computations, the perfectly matched layer (PML) absorbing boundaries are used for the truncation of the computation domain. A symmetric GaAs-based dielectric slab waveguide is considered to test the proposed FDTD algorithm. It consists of a 0.44-μm-thick guiding layer sandwiched between two 3-μm-thick AlAs layers. The arrangements of the field components for both the fundamental and second harmonic are made according to the standard Yee cell. The excitation field is a continuous-wave transverse-magnetic (TM) signal (H_y) at a fundamental wavelength of $\lambda_f = 1.064$ μm and an amplitude of 5.0 A/μm. The transverse profile of the excitation corresponds to the first TM guided mode at the given operating frequency. The nonlinear susceptibility is taken as $\chi^{(2)} = 113$ pm/V. A long simulation time corresponding to tens of cycles was allowed to ensure steady-state results. The mesh parameters were carefully chosen to effectively reduce numerical dispersion especially in the propagation direction. The algorithm is tested for several matching scenarios. First, no matching is considered such that the level of coupling between the input and the generated waves depends entirely

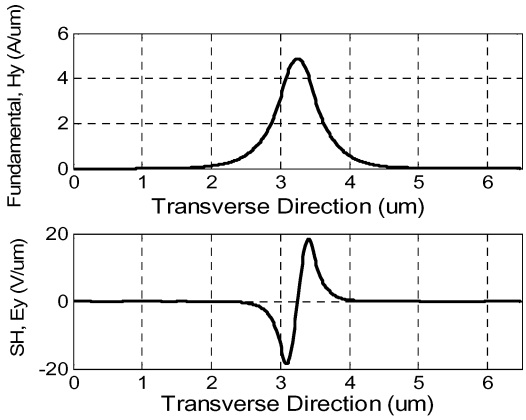

Fig. 1. Transverse profiles of the TM input (fundamental) and generated TE second-harmonic fields.

$$E_y^{s(n+1)}(i,j) = E_y^{s(n)}(i,j) + \frac{\Delta t}{\varepsilon_y(i,j)} \left[\left(\frac{H_x^{s(n+\frac{1}{2})}\left(i, j+\frac{1}{2}\right) - H_x^{s(n+\frac{1}{2})}\left(i, j-\frac{1}{2}\right)}{\Delta z} \right) + \left(\frac{H_z^{s(n+\frac{1}{2})}\left(i+\frac{1}{2}, j\right) - H_z^{s(n+\frac{1}{2})}\left(i-\frac{1}{2}, j\right)}{\Delta x} \right) \right] - \frac{2\varepsilon_0 d_{14} \Delta t}{\varepsilon_y(i,j)} \cdot \left(\frac{T^{n+1} - T^n}{\Delta t} \right) \tag{12}$$

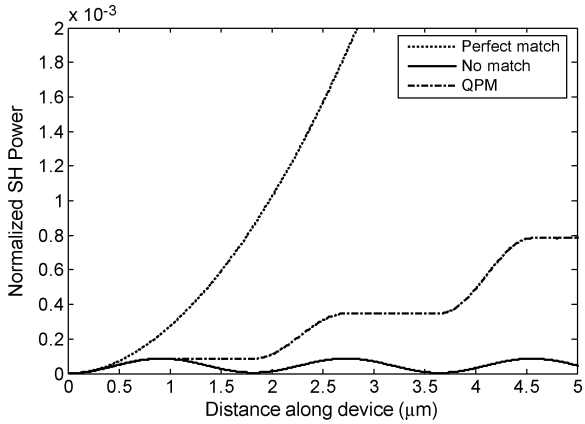

Fig. 2. Normalized SH power along the nonlinear waveguide (solid line: no matching; dotted line: perfect match; dotted–dashed line: QPM.

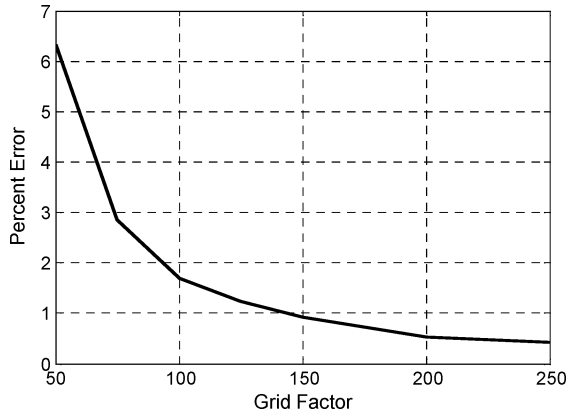

Fig. 3. Percent error in simulated coherence length versus the grid factor.

on the phase difference between them. This phase difference is defined by the effective indices of the two coexisting guided modes. The transverse profiles for the fundamental TM mode and the second-harmonic transverse-electric (TE) mode are shown in Fig. 1. The simulation verifies the coupling of second-harmonic energy on the first odd TE mode. Second, the effective refractive index of the first odd guided mode of the TE field at $\lambda_s = 0.532\ \mu$m is perfectly matched to the first even guided mode of the TM input field by numerically changing the value of the refractive index of the guiding layer at λ_s. Third, the quasi-phase-matching (QPM) technique is implemented by alternately switching the nonlinearity ON and OFF along the waveguide with periodicity equal to the coherence period $\Lambda_c = \lambda_f/2(n_{\text{eff}}^s - n_{\text{eff}}^f)$. The normalized SH power curves for all scenarios are shown in Fig. 2. As expected, energy exchange between the fundamental field and the second-harmonic field takes place periodically during every coherence period if no matching technique is implemented. If, however, the two waves are perfectly matched, the energy exchange will be continuous, resulting in a coherent build-up of the second-harmonic energy. The analytical value of the coherence length $(\Lambda_c/2)$ is used to test the convergence of the algorithm. Fig. 3 shows the percent error in the simulated values of the coherence length versus the grid factor which is defined as the number of grid points per one wavelength. The percent error is defined as $(\Lambda_c^{\text{analytical}} - \Lambda_c^{\text{simulated}}) \times 100/\Lambda_c^{\text{analytical}}$. The proposed FDTD algorithm produces errors of less than 0.5% for grid factors around 200.

IV. Conclusion

A new vectorial nonparaxial FDTD algorithm to model SHG in nonlinear optical devices has been proposed and tested. The developed model can be utilized to efficiently analyze and study different optical structures. The extension of the model to applications involving pulsed excitations and different device nonlinearities is a future work.

References

[1] H. Masoudi and J. Arnold, "Modeling second-order nonlinear effects in optical waveguides using a parallel-processing beam propagation method," *IEEE J. Quantum Electron.*, vol. 31, no. 12, pp. 2107–2113, Dec. 1995.

[2] T. Yasui and M. Koshiba, "Three-dimensional vector beam-propagation method for second harmonic generation analysis," *J. Lightw. Technol.*, vol. 19, no. 5, pp. 780–785, May 2001.

[3] F. A. Katsriku, B. M. A. Rahman, and K. T. V. Grattan, "Finite-element analysis of second-harmonic generation in AlGaAs waveguides," *IEEE J. Quantum Electron.*, vol. 36, no. 3, pp. 282–289, Mar. 2000.

[4] R. Joseph and A. Taflove, "FDTD Maxwell's equations models for nonlinear electrodynamics and optics," *IEEE Trans. Antenna Propagat.*, vol. 45, no. 3, pp. 364–374, Mar. 1997.

[5] M. A. Alsunaidi, H. M. Masoudi, and J. M. Arnold, "A time-domain algorithm for second harmonic generation in nonlinear optical structures," *IEEE Photon. Technol. Lett.*, vol. 12, no. 4, pp. 395–397, 2000.

[6] T. Lee and S. C. Hagness, "Pseudospectral time-domain methods for modeling optical wave propagation in second-order nonlinear materials," *J. Opt. Soc. Amer. B.*, vol. 21, pp. 330–342, 2004.

[7] C. M. Reinke, A. Jafarpour, B. Momeni, M. Soltani, S. Khorasani, A. Adibi, Y. Xu, and R. K. Lee, "Nonlinear finite-difference time-domain method for the simulation of anisotropic, $\chi^{(2)}$, and $\chi^{(3)}$ optical effects," *J. Lightw. Technol.*, vol. 24, no. 1, pp. 624–634, Jan. 2006.